

Synthesis, Crystal Structure and Characterisation of a Novel Chiral Mixed-Valence Vanadium Oxide Hybrid, $[V_5O_{11}(\text{dien})_3]$

Ming-Lai Fu,^[a,b] Guo-Cong Guo,^{*[a]} A-Qing Wu,^[a] Bin Liu,^[a] Li-Zhen Cai,^[a] and Jin-Shun Huang^[a]

Keywords: Chirality / dien ligand / Magnetism / Mixed-valence compounds / Vanadium

The novel chiral mixed-valence vanadium oxide hybrid $[V_5O_{11}(\text{dien})_3]$ (**1**) (dien = $\text{NH}_2\text{C}_2\text{H}_4\text{NHC}_2\text{H}_4\text{NH}_2$) has been synthesised by a hydrothermal reaction of V_2O_5 and dien in aqueous solution and characterised by elemental analysis, IR spectroscopy, TG-DSC analysis, magnetism, EPR spectroscopy, single-crystal X-ray diffraction and powder XRD. The X-ray diffraction analysis revealed that the structure of **1** can be regarded as being constructed from two $[V^VO_4]^{3-}$ groups bicapping three $[V^{IV}O(\text{dien})]^{2+}$ units to form a discrete asymmetric pentanuclear vanadium complex with the

dien ligands coordinating directly to the vanadium(IV) centres. Compound **1** exhibits an interesting tube-like 3D supramolecular structure due to abundant hydrogen-bonding interactions between the oxygen atoms of the inorganic backbone and the hydrogen atoms of the dien ligands from adjacent molecules. The variable-temperature magnetic susceptibility data of **1** suggest a weak ferromagnetic interaction among V^{4+} ions in the cluster.

(© Wiley-VCH Verlag GmbH & Co. KGaA, 69451 Weinheim, Germany, 2005)

Introduction

Increasing attention has been paid to inorganic oxides due to their structural diversity and applications in the fields of catalysis, sorption, electrical conductivity, magnetism and photochemistry^[1] and the synthesis of new materials possessing unique structures and properties based on inorganic oxides remains a challenge. The role of organic components on the structural modification of inorganic oxides has been well recognised in recent years.^[2] Generally, the organic components act as structural directors to tune inorganic frameworks, compensate charges and fill space. On the other hand, they may also function as ligands coordinated directly to the oxide scaffolding or to the secondary metal centres.^[3] Recently, the introduction of the hydrothermal technique and the use of organic structure-directing agents has led to the production of various vanadium oxide discrete clusters with 1D, 2D and 3D structures.^[4] A large family of inorganic-organic hybrids based on the vanadium oxides has been investigated using organic amines as organic components in which the amines are usually protonated and intercalated between the anionic vanadium oxide layers.^[5] However, the investigations of amines as ligands coordinated directly to vanadium centres has been lim-

ited.^[6] We are interested in introducing transition metal-amine complexes into the inorganic framework and understanding the role of metal complexes on the modification of inorganic framework structures.^[7] Herein, we report a novel chiral mixed-valence vanadium oxide, $[V_5O_{11}(\text{dien})_3]$ (**1**), with the achiral tridentate dien ligands coordinated directly to the vanadium(IV) centres.

Results and Discussion

The title hybrid was prepared from V_2O_5 (0.182 g, 1 mmol), dien (4 mL) and H_2O (6 mL) under hydrothermal conditions in a 25-mL capacity Teflon-lined steel autoclave at 160 °C for 6 d. The dien in the reaction acts not only as an agent for reducing V^{5+} to V^{4+} but also as a ligand coordinated to V^{4+} . Furthermore, it is an organic base to adjust the pH value of the aqueous solution in order to maintain strongly basic conditions during the whole synthesis which plays a significant role in the formation of **1**. Detailed experiments suggest that excess dien is necessary to yield **1** using V_2O_5 as a starting material and it failed to form if the amount of dien was less than 3.5 mL or if NH_4VO_3 was used as a starting material instead (Table S1; see supporting information, for supporting information see also the footnote on the first page of this article).

A single-crystal X-ray analysis reveals that **1** consists of a chiral mixed-valence vanadium oxide hybrid $[V_5O_{11}(\text{dien})_3]$ (Figure 1). The asymmetric pentanuclear vanadium cluster exhibits two types of vanadium coordination envi-

[a] State Key Laboratory of Structural Chemistry, Fujian Institute of Research on the Structure of Matter, Chinese Academy of Sciences, Fuzhou, Fujian 350002, P. R. China
E-mail: gcguo@ms.fjirsm.ac.cn

[b] Graduate School of Chinese Academy of Sciences, Beijing 100039, P. R. China

Supporting information for this article is available on the WWW under <http://www.eurjic.org> or from the author.

ronments in which the V(4) and V(5) atoms are in distorted VO_4 tetrahedra and the V(1), V(2) and V(3) atoms exhibit distorted VO_3N_3 octahedral geometries. In the VO_4 tetrahedron, the vanadium centre is coordinated by three bridging oxygen atoms (O_b) and one terminal oxygen atom (O_t). The V– O_b bond lengths are in the range of 1.708(1)–1.743(1) Å, the V– O_t bond lengths are 1.658(2) and 1.662(2) Å and the O–V–O bond angles range from 107.9(1) to 113.0(1)°. In the VO_3N_3 octahedron, each V atom is chelated by one dien ligand in a tridentate manner and in a facial configuration with the V–N bond lengths ranging from 2.137(2) to 2.339(2) Å and coordinated by one O_t atom and two O_b atoms from two VO_4 tetrahedra. The V– O_b bond lengths range from 1.925(1) to 1.966(1) Å and the V– O_t bond lengths are in the range of 1.611(2)–1.621(2) Å thereby form a distorted octahedron with a π configuration^[8] in which the three dien ligands coordinated to V1, V2 and V3 exhibit $\delta\delta$, $\lambda\lambda$ and $\delta\delta$ conformations, respectively. The significantly distorted V octahedra are evident from the axial angles which range from 158.3(1) to 164.5(1)°. Bond-valence sum (BVS) calculations^[9] [V(1) = 4.066, V(2) = 4.057, V(3) = 3.999, V(4) = 5.179, V(5) = 5.160] show that the V octahedra are occupied by V^{4+} ions and the V tetrahedra by V^{5+} ions which is consistent with the overall charge balance of the compound. Magnetic measurements support the BVS calculations for the valence assignment of V atoms (see below). The five vanadium atoms in the pentanuclear cluster can be described as a giant trigonal bipyramid with three V^{4+} atoms lying on the equatorial plane and two V^{5+} atoms occupying the axial positions in which two $[\text{VO}_4]^{3-}$ groups are bicapping the $[\text{VO}(\text{dien})]^{2+}$ unit through corner-sharing their polyhedra (Figure S1). The present mixed-valence pentanuclear vanadium hybrid has been found for the first time in the neutral form, although mixed-valence pentanuclear vanadium compounds have been previously characterised as anions in $[\text{Et}_4\text{N}]_2[\text{V}_5\text{O}_9\text{X}(\text{O}_2\text{CR})_4]$ salts ($\text{X} = \text{Cl}^-$, Br^- ; $\text{R} = \text{Ph}$, CH_3).^[10]

An interesting feature is that the space group of **1** is $P6_3$ which results in its chiral nature. In recent years, much effort has been devoted to the controlled construction of inorganic coordination compounds with enantiopure topologies, stimulated by their potential impact on important areas of research such as enantioselective catalysis and molecular recognition. Achiral molecules^[11] as well as chiral species^[12] can be used to synthesise chiral coordination compounds. However, the achiral approach almost always leads to a racemic mixture^[13] and it is not well understood how homochiral packing in crystals can be induced.^[14] Although the inorganic V_5O_{11} backbone and the dien ligand in **1** are achiral, the homochiral structure of **1** is induced by the different twist of the organic ligand chelating to the vanadium(IV) centres. The powder XRD pattern of **1** and the pattern simulated on the basis of the single-crystal structure are presented in Figure 2. The diffraction peaks in both patterns correspond well in their positions, indicating the phase purity of the prepared sample. In the IR spectrum of **1** (Figure S2, supporting information), the strong bands at 967, 867, 832, 735 and 675 cm^{-1} are due to the

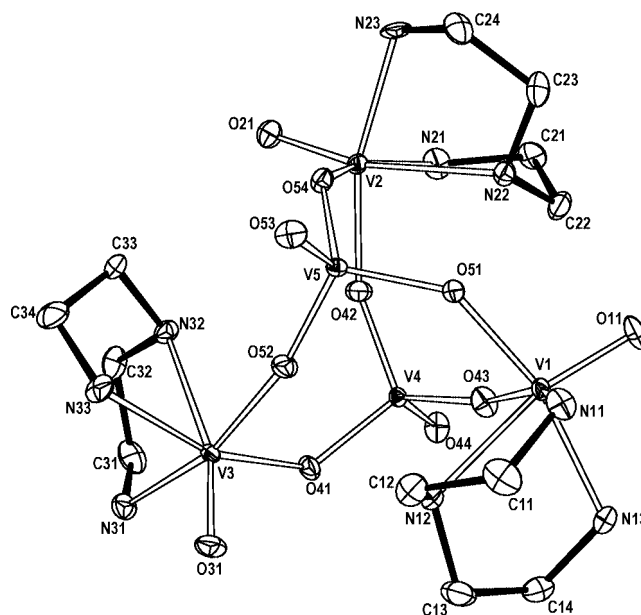


Figure 1. Molecular structure of **1** with 30% thermal ellipsoids. Hydrogen atoms are omitted for clarity.

terminal V=O stretch and the V–O–V stretch. Bands in the 1107–1619 cm^{-1} region can be attributed to characteristic peaks of the dien ligand.

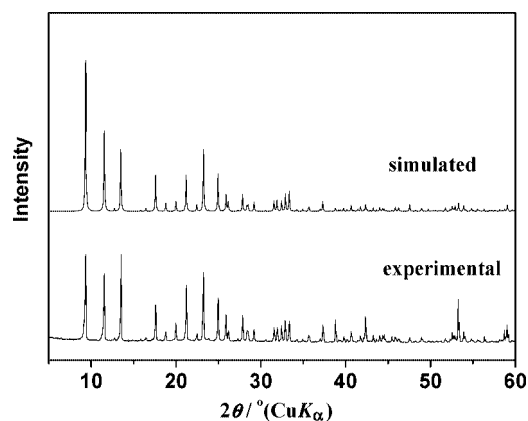


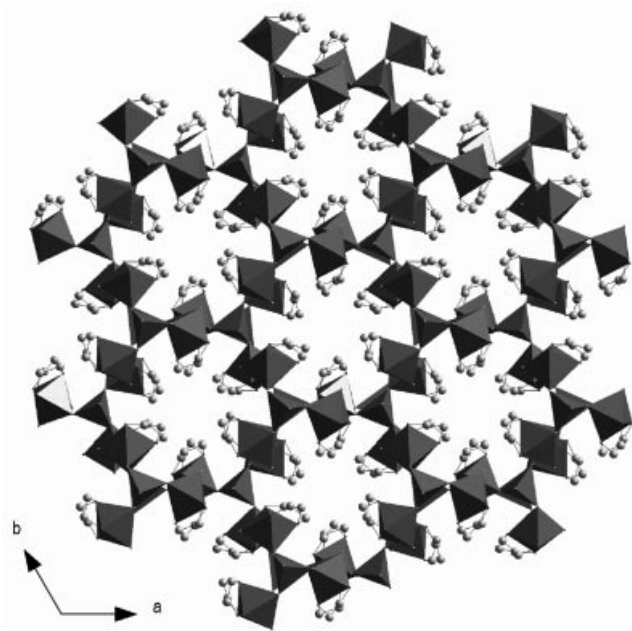
Figure 2. Experimental and simulated powder X-ray diffraction pattern of **1**.

As shown in Figure 3, the $[\text{V}_5\text{O}_{11}(\text{dien})_3]$ molecules are stably packed together to exhibit an interesting tube-like 3D supramolecular array with 1D channels (about 2.4 Å in free diameter, Figure S3, supporting information) along the c direction by means of abundant hydrogen-bonding interactions between the oxygen atoms of vanadium oxides and the hydrogen atoms of dien ligands from adjacent molecules (Table 1; Figures S4 and S5, supporting information). It is of note that the hydrogen-bonding interactions play a significant role in the stabilisation of the structure of **1** which is consistent with the thermal analysis experiments. The TGA and DSC data, recorded from 30 to 1000 °C under flowing N_2 , show that the weight of **1** is almost unchanged

Table 1. Hydrogen bond lengths [Å] and angles [°] of complex **1**.

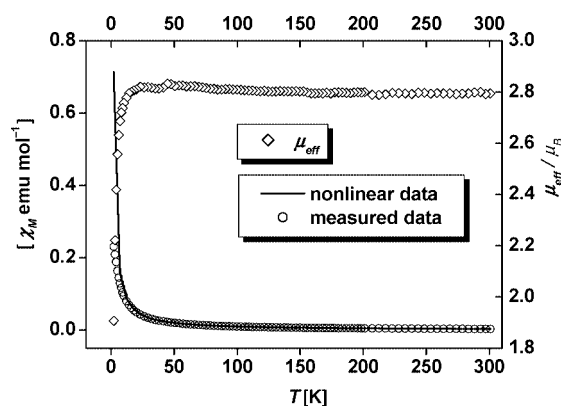
Atom involved	Distance (N...O)	Angles N–H...O	Symmetry-equivalent operations
N11–H11D...O41_1	3.040(2)	139.1	\$1: y, -x + y
N11–H11C...O44_1	2.944(2)	112.7	
N13–H13D...O31_2	3.001(2)	159.2	\$2: -x + y, -x, z
N13–H13C...O53_3	2.940(2)	150.9	\$3: y, -x + y, -0.5 + z
N21–H21D...O53_4	2.938(2)	167.9	\$4: -x, 1 - y, -0.5 + z
N23–H23D...O11_5	2.913(2)	160.9	\$5: -x + y, 1 - x, z
N23–H23C...O44_6	2.876(2)	157.6	\$6: -x, 1 - y, 0.5 + z
N31–H31D...O21_7	2.984(2)	161.0	\$7: -1 - x + y, -x, z
N31–H31C...O53_8	2.969(2)	152.5	\$8: x - y, x, -0.5 + z
N33–H33C...O44_9	2.904(2)	142.0	\$9: x - y, x, 0.5 + z

from 30 to 260 °C (Figure S7). In the range of 260–400 °C the main weight loss occurs which is associated with two endothermic peaks and should be due to the loss of organic molecules. The endothermic peaks in this weight-loss stage imply that there exist strong coordination bonds between the V centre and the dien ligand and abundant hydrogen bonds in **1**. The observed weight loss (42.15%) is close to that which would result from losing three dien molecules per empirical formula unit (41.81%). The TGA chart shows that the next weight loss (7.99%) in the range of 400–800 °C may be due to the emission of oxygen to yield V_2O_3 as a residue (calcd. 7.57%).

Figure 3. Polyhedral representation of **1** as a packed view along the *c* direction showing the tube-like structure.

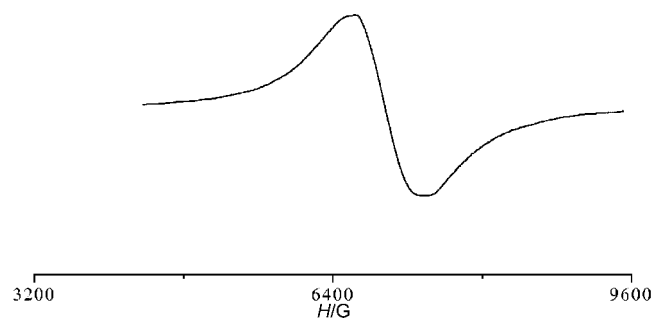
The variable-temperature magnetic susceptibility data of **1** were recorded on a crystalline sample in a field of 1 T and in the 2–300 K temperature range as shown in Figure 4 in the χ_M and μ_{eff} vs. *T* plots. The data were fitted using the Curie-Weiss equation above 75 K: $\chi_M = C/(T - \theta) + \chi_0$, $\chi_0 = -3.6(1) \times 10^{-4} \text{ emu mol}^{-1}$, $C = 0.970(3) \text{ emu K mol}^{-1}$ and $\theta = 1.6(2) \text{ K}$. The effective magnetic moment, calculated from the equation $\mu_{\text{eff}} = 2.828 C^{1/2}$ is $2.8(2) \mu_B$ which is close to the value of $3 \mu_B$ for three independent unpaired electrons

per formula unit. The slow increases in the μ_{eff} value with the decreasing temperature of **1** and a small positive θ clearly indicate the presence of weak ferromagnetic interactions among the V^{4+} ions in **1**. To simulate the experimental magnetic behaviour, we used the analytical experimental expression deduced for trinuclear magnetic metal atoms in compounds with classical spins.^[15]

Figure 4. χ_M vs. *T* and μ_{eff} vs. *T* plots for **1**. The solid lines represent the nonlinear curve fit of the experimental data.

$$\chi_M = \frac{N\beta^2 g^2}{4kT} \frac{1 + 5\exp(3J/2kT)}{1 + \exp(3J/2kT)}$$

In this expression, *N* is Avogadro's number, β is Bohr's magneton and *k* is Boltzmann's constant. The best least-squares fit of the theoretical equation to experimental data leads to $g = 1.8570(6)$, $J/k = 3.3(1) \text{ K}$ and the agreement factor $R = 1.02 \times 10^{-5}$ [$R = \Sigma [(\chi_M T)_{\text{obsd.}} - (\chi_M T)_{\text{calcd.}}]^2 / \Sigma [(\chi_M T)_{\text{obsd.}}]^2$]. The positive *J* value suggests that a weak ferromagnetic interaction exists in **1** which is in agreement with the result of the fit obtained from the Curie-Weiss law. Unlike the vast majority of known polynuclear vanadium(IV) or -(IV/V) compounds which exhibit antiferromagnetic coupling between V^{IV} magnetic ions,^[16] the present chiral pentanuclear vanadium(IV/V) compound shows ferromagnetic behaviour. The EPR spectrum of **1** (Figure 5) at room temperature shows a V^{4+} signal with $g = 1.9543$ which is consistent with the value obtained from the fitting of the magnetic susceptibility data.

Figure 5. Powder X-band EPR spectrum of **1**.

Conclusions

In conclusion, a novel chiral mixed-valence vanadium oxide hybrid, $[V_5O_{11}(\text{dien})_3]$, in which the dien ligands are chelated to vanadium(IV) centres in a tridentate manner has been successfully synthesised by a hydrothermal process. This result shows that the chiral hybrid can be constructed from achiral starting materials which are induced by the different twist of the organic ligands chelating to the vanadium(IV) centres. The material exhibits an interesting tube-like channel structure resulting from abundant intermolecular hydrogen bonding interactions and shows weak ferromagnetic interactions.

Experimental Section

General Remarks: All reagents were purchased from commercial sources and used without further purification. Elemental analyses (C, H, N and O) were performed with an Elementar Vario EL III microanalyser. The infrared spectrum was recorded as a KBr pellet in the range of 4000–400 cm^{-1} with a Nicolet FTIR Magna 750

spectrophotometer. The powder X-ray diffraction pattern was collected with a Rigaku DMAX2500 diffractometer at 40 kV and 100 mA for $\text{Cu-K}\alpha$ ($\lambda = 1.5406 \text{ \AA}$), with a scan speed of 5°min^{-1} at room temperature. The simulated pattern was produced using the Platon program and single-crystal reflection data. A Netzsch STA 449C thermogravimetric analyser was used to obtain TGA and DSC curves under N_2 with a temperature increment of $10^\circ \text{C min}^{-1}$ in the temperature range 30–1000 $^\circ \text{C}$. An empty Al_2O_3 crucible was used as a reference.

$[V_5O_{11}(\text{dien})_3]$ (1**):** Powdery V_2O_5 (0.182 g, 1 mmol) was added to a solution of dien (4 mL) in H_2O (6 mL). The mixture was stirred at room temperature for 1 h then transferred into a 25-mL teflon-lined stainless steel autoclave and heated at 160 $^\circ \text{C}$ under autogeneous pressure for 6 d. After cooling, the brown crystals obtained by filtration were washed with water and ethanol. Yield: 80% (based on V_2O_5). $\text{C}_{12}\text{H}_{39}\text{N}_9\text{O}_{11}\text{V}_5$ (740.2): calcd. C 19.47, H 5.31, N 17.03, O 23.78; found C 19.33, H 5.06, N 17.08, O 23.70.

Table 3. Selected bond lengths [\AA] for compound **1**.

V(1)–O(11)	1.6188(12)	V(3)–O(52)	1.9349(13)
V(1)–O(43)	1.9245(14)	V(3)–O(41)	1.9559(13)
V(1)–O(51)	1.9569(15)	V(3)–N(31)	2.1374(16)
V(1)–N(13)	2.1456(18)	V(3)–N(33)	2.1940(18)
V(1)–N(11)	2.1668(18)	V(3)–N(32)	2.3385(18)
V(1)–N(12)	2.3096(13)	V(4)–O(44)	1.6583(17)
V(2)–O(21)	1.6112(15)	V(4)–O(42)	1.7172(15)
V(2)–O(42)	1.9372(14)	V(4)–O(43)	1.7172(13)
V(2)–O(54)	1.9560(14)	V(4)–O(41)	1.7427(11)
V(2)–N(23)	2.1490(15)	V(5)–O(53)	1.6622(16)
V(2)–N(21)	2.1695(17)	V(5)–O(52)	1.7077(12)
V(2)–N(22)	2.3305(17)	V(5)–O(54)	1.7321(13)
V(3)–O(31)	1.6208(16)	V(5)–O(51)	1.7380(12)

Table 4. Selected bond angles [$^\circ$] for compound **1**.

O(11)–V(1)–O(43)	105.93(7)	N(21)–V(2)–N(22)	74.93(6)
O(11)–V(1)–O(51)	102.47(7)	O(31)–V(3)–O(52)	105.42(7)
O(43)–V(1)–O(51)	91.26(6)	O(31)–V(3)–O(41)	104.93(7)
O(11)–V(1)–N(13)	93.61(7)	O(52)–V(3)–O(41)	88.33(6)
O(43)–V(1)–N(13)	88.16(7)	O(31)–V(3)–N(31)	94.66(7)
O(51)–V(1)–N(13)	163.41(5)	O(52)–V(3)–N(31)	159.86(7)
O(11)–V(1)–N(11)	95.78(7)	O(41)–V(3)–N(31)	87.98(6)
O(43)–V(1)–N(11)	158.29(5)	O(31)–V(3)–N(33)	94.14(7)
O(51)–V(1)–N(11)	83.85(7)	O(52)–V(3)–N(33)	81.71(6)
N(13)–V(1)–N(11)	90.58(7)	O(41)–V(3)–N(33)	160.29(6)
O(11)–V(1)–N(12)	164.54(8)	N(31)–V(3)–N(33)	95.52(7)
O(43)–V(1)–N(12)	83.65(5)	O(31)–V(3)–N(32)	163.37(6)
O(51)–V(1)–N(12)	89.18(5)	O(52)–V(3)–N(32)	85.76(6)
N(13)–V(1)–N(12)	74.27(6)	O(41)–V(3)–N(32)	87.37(6)
N(11)–V(1)–N(12)	75.17(6)	N(31)–V(3)–N(32)	74.30(6)
O(21)–V(2)–O(42)	103.22(7)	N(33)–V(3)–N(32)	75.02(6)
O(21)–V(2)–O(54)	105.48(7)	O(44)–V(4)–O(42)	109.16(7)
O(42)–V(2)–O(54)	90.22(6)	O(44)–V(4)–O(43)	107.86(7)
O(21)–V(2)–N(23)	94.48(7)	O(42)–V(4)–O(43)	109.92(7)
O(42)–V(2)–N(23)	162.18(6)	O(44)–V(4)–O(41)	108.12(6)
O(54)–V(2)–N(23)	87.08(6)	O(42)–V(4)–O(41)	108.74(6)
O(21)–V(2)–N(21)	94.16(7)	O(43)–V(4)–O(41)	112.97(6)
O(42)–V(2)–N(21)	84.42(6)	O(53)–V(5)–O(52)	108.72(6)
O(54)–V(2)–N(21)	160.34(6)	O(53)–V(5)–O(54)	108.26(7)
N(23)–V(2)–N(21)	92.26(6)	O(52)–V(5)–O(54)	111.94(7)
O(21)–V(2)–N(22)	163.41(6)	O(53)–V(5)–O(51)	109.63(7)
O(42)–V(2)–N(22)	88.37(6)	O(52)–V(5)–O(51)	107.92(7)
O(54)–V(2)–N(22)	86.04(5)	O(54)–V(5)–O(51)	110.33(6)
N(23)–V(2)–N(22)	73.88(6)		

Table 2. Crystal data and structural refinements details for complex **1**.

Empirical formula	$\text{C}_{12}\text{H}_{39}\text{N}_9\text{O}_{11}\text{V}_5$
Formula mass [g mol^{-1}]	740.22
Crystal colour	brown
Crystal habit	chip
Crystal size [mm]	$0.30 \times 0.30 \times 0.22$
Crystal system	hexagonal
Space group	$P6_3$
a [\AA]	18.8426(5)
c [\AA]	13.0627(7)
V [\AA^3]	4016.5(3)
Z	6
λ (Mo- $K\alpha$) [\AA]	0.71073
$D_{\text{calcd.}}$ [g cm^{-3}]	1.836
μ (Mo- $K\alpha$) [mm^{-1}]	1.747
$F(000)$	2262
Flack parameter	0.0(2)
2θ range [$^\circ$]	3.30 to 25
Reflections collected	29579
Independent reflections	4349
Observed data [$I > 2\sigma(I)$]	4084
R_{int}	0.0377
R indexes [$I > 2\sigma(I)$]	$R_1 = 0.0334$, $wR_2 = 0.0831$
R indexes (for all reflections)	$R_1 = 0.0372$, $wR_2 = 0.0851$
Goodness of fit	0.997
Largest difference peak and hole [e \AA^{-3}]	0.306, -0.284

X-ray Crystallographic Study: The single-crystal X-ray data for **1** were collected with a Rigaku Mercury CCD diffractometer with graphite-monochromated Mo- K_{α} radiation using the ω -scan technique at 293 K and CrystalClear^[17] software was used for data reduction. The structure was solved by direct methods using the Siemens SHELXTLTM Version 5 crystallographic software package.^[18] The difference Fourier maps based on these atomic positions yielded the other non-hydrogen atoms and the hydrogen atoms bound to nitrogen atoms. The structure was refined using a full-matrix least-squares refinement on F^2 . All non-hydrogen atoms were refined anisotropically. The positions of hydrogen atoms bound to carbon atoms were generated symmetrically, allowed to ride on their respective parent atoms and included in the structure factor calculations with assigned isotropic thermal parameters but were not refined. Crystallographic data are summarised in Table 2 and selected bond lengths and angles are listed in Tables 3 and 4. CCDC-260926 contains the supplementary crystallographic data for this paper. These data can be obtained free of charge from the Cambridge Crystallographic Data Centre via www.ccdc.cam.ac.uk/data_request/cif.

Supporting Information (see also footnote on the first page of this article): Details of the compositions of reactants for the preparation of **1**, DSC and TG curves, IR spectra and crystal structural diagrams indicating hydrogen bonds.

Acknowledgments

We gratefully acknowledge the financial support of the NSF of China (20131020), the NSF for Distinguished Young Scientist of China (20425104) and the NSF of Fujian Province (20031031).

- [1] a) A. K. Cheetham, *Science* **1994**, *264*, 794 and references cited therein; b) P. A. Cox, *Transition Metal Oxides*, Clarendon Press, Oxford, **1995**; c) A. Müller, H. Reuter, S. Dillinger, *Angew. Chem. Int. Ed. Engl.* **1995**, *34*, 2328; d) M. T. Pope, A. Müller, *Angew. Chem. Int. Ed. Engl.* **1991**, *30*, 34; e) M. T. Pope, *Heteropoly and Isopoly Oxometalates*, Springer, New York, **1983**; f) A. Müller, F. Peters, M. T. Pope, D. Gatteschi, *Chem. Rev.* **1998**, *98*, 239; g) A. Clearfield, *Chem. Rev.* **1988**, *88*, 125; h) P. J. Hagrman, D. Hagrman, J. Zubieta, *Angew. Chem. Int. Ed.* **1999**, *38*, 2638.
- [2] a) S. I. Stupp, P. V. Braun, *Science* **1997**, *277*, 1242; b) O. M. Yaghi, H. Li, C. Davis, D. Richardson, T. L. Groy, *Acc. Chem. Res.* **1998**, *31*, 474; c) S. R. Batten, R. Robson, *Angew. Chem. Int. Ed.* **1998**, *37*, 1460; d) P. V. Braun, P. Osenar, V. Tohver, S. B. Kennedy, S. I. Stupp, *J. Am. Chem. Soc.* **1999**, *121*, 7302.
- [3] P. J. Hagrman, J. Zubieta, *Inorg. Chem.* **2000**, *39*, 3260.
- [4] a) Y. Zhang, P. J. Zapf, L. M. Meyer, R. C. Haushalter, J. Zubieta, *Inorg. Chem.* **1997**, *36*, 2159; b) L. M. Zheng, J. S. Zhao, K. H. Li, L. Y. Zhang, Y. Liu, X. Q. Xin, *J. Chem. Soc. Dalton Trans.* **1999**, 939; c) L. R. Zhang, Z. Shi, G. Y. Yang, X. M. Chen, S. H. Feng, *J. Chem. Soc. Dalton Trans.* **2000**, 275; d) X. M. Zhang, M. L. Tong, X. M. Chen, *Chem. Commun.* **2000**, 1817; e) J. Tao, X. M. Zhang, M. L. Tong, X. M. Chen, *J. Chem. Soc. Dalton Trans.* **2001**, 770; f) C. M. Liu, S. Gao, H. Z. Kou, *Chem. Commun.* **2001**, 1670; g) J. Do, A. J. Jacobson, *Inorg. Chem.* **2001**, *40*, 2468; h) P. J. Hagrman, J. Zubieta, *Inorg. Chem.* **2001**, *40*, 2800; i) C. M. Liu, Y. L. Hou, J. Zhang, S. Gao, *Inorg. Chem.* **2002**, *41*, 140; j) Y. Lu, E. B. Wang, M. Yuan, G. Y. Luan, Y. G. Li, H. Zhang, C. W. Hu, Y. G. Yao, Y. G. Qin, Y. B. Chen, *J. Chem. Soc. Dalton Trans.* **2002**, 3029.
- [5] a) D. Riou, G. Férey, *J. Solid State Chem.* **1995**, *120*, 137; b) L. F. Nazar, B. E. Koene, J. F. Britten, *Chem. Mater.* **1996**, *8*, 327; c) Y. P. Zhang, C. J. O'Connor, A. Clearfield, R. C. Haushalter, *Chem. Mater.* **1996**, *8*, 595; d) Y. P. Zhang, R. C. Haushalter, A. Clearfield, *Chem. Commun.* **1996**, 1055; e) J. Livage, *Coord. Chem. Rev.* **1998**, *178*, 999; f) T. Chirayil, P. Y. Zavalij, M. S. Whittingham, *Chem. Mater.* **1998**, *10*, 2629; g) P. Zavalij, M. S. Whittingham, *Acta Crystallogr. Sect. B* **1999**, *55*, 627.
- [6] a) K. Wiegardt, M. Koppen, B. Nuber, J. Weiss, *J. Chem. Soc. Chem. Commun.* **1986**, 1530; b) R. Hotzelmann, K. Wiegardt, U. Florke, H.-J. Haupt, *Angew. Chem. Int. Ed. Engl.* **1990**, *29*, 645; c) J. G. Reynolds, S. C. Sendlinger, A. M. Murray, J. C. Huffman, G. Christou, *Angew. Chem. Int. Ed. Engl.* **1992**, *31*, 1253; d) W. Plass, J. G. Verkade, *J. Am. Chem. Soc.* **1992**, *114*, 2275; e) D. Reardon, J. Guan, S. Gambarotta, G. P. A. Yap, D. R. Wilson, *Organometallics* **2002**, *21*, 4390; f) M. P. Shores, J. R. Long, *J. Am. Chem. Soc.* **2002**, *124*, 3512.
- [7] a) M.-L. Fu, G.-C. Guo, X. Liu, B. Liu, L.-Z. Cai, J.-S. Huang, *Inorg. Chem. Commun.* **2005**, *8*, 18; b) M.-L. Fu, G.-C. Guo, L. Z. Cai, Z.-J. Zhang, J.-S. Huang, *Inorg. Chem.* **2005**, *44*, 184.
- [8] a) A. R. Gainsford, D. A. House, *Inorg. Chim. Acta* **1969**, *3*, 367; b) A. R. Gainsford, D. A. House, W. T. Robinson, *Inorg. Chim. Acta* **1971**, *5*, 595.
- [9] a) I. D. Brown, D. Altermatt, *Acta Crystallogr. Sect. B* **1985**, *41*, 244; b) N. E. Brese, M. O. Keefe, *Acta Crystallogr. Sect. B* **1991**, *47*, 192.
- [10] a) G. B. Karet, Z. Sun, D. D. Heinrich, J. K. McCusker, K. Foltz, W. E. Streib, J. C. Huffman, D. N. Hendrickson, G. Christou, *Inorg. Chem.* **1996**, *35*, 6450; b) G. B. Karet, Z. Sun, W. E. Streib, J. C. Bollinger, D. N. Hendrickson, G. Christou, *Chem. Commun.* **1999**, 2249.
- [11] a) D. Rabinovich, B. S. Green, M. Lahav, *Acc. Chem. Res.* **1979**, *12*, 191; b) T. Ezuhara, K. Endo, Y. Aoyama, *J. Am. Chem. Soc.* **1999**, *121*, 3279; c) M. A. Withersby, A. J. Blake, N. R. Champness, P. Hubberstey, W.-S. Li, M. Schröder, *Angew. Chem. Int. Ed. Engl.* **1997**, *36*, 2327; d) S. R. Batten, B. F. Hoskins, R. Robson, *Angew. Chem. Int. Ed. Engl.* **1997**, *36*, 636; e) R. Krämer, J.-M. Lehn, A. De Cian, J. Fischer, *Angew. Chem. Int. Ed. Engl.* **1993**, *32*, 703.
- [12] a) F. R. Keene, *Coord. Chem. Rev.* **1997**, *166*, 121; b) U. Knof, A. von Zelewsky, *Angew. Chem. Int. Ed.* **1999**, *38*, 302.
- [13] O. J. Gelling, F. Van Bolhuis, B. L. Feringa, *J. Chem. Soc. Chem. Commun.* **1991**, 917.
- [14] a) H. Koshima, E. Hayashi, K. Matsuura, K. Tanaka, F. Toda, M. Kato, M. Kiguchi, *Tetrahedron Lett.* **1997**, *38*, 5009; b) D. K. Kondepudi, R. J. Kaufman, N. Singh, *J. Am. Chem. Soc.* **1993**, *115*, 10211; c) J. M. McBride, R. L. Carter, *Angew. Chem. Int. Ed. Engl.* **1991**, *30*, 293; d) D. K. Kondepudi, R. J. Kaufman, N. Singh, *Science* **1990**, *250*, 975.
- [15] O. Kahn, *Molecular Magnetism*, VCH, Weinheim, Germany, **1993**.
- [16] a) J. M. Clemente-Juan, E. Coronado, *Coord. Chem. Rev.* **1999**, *193–195*, 361 and references cited therein; b) A. Müller, F. Peters, M. T. Pope, D. Gatteschi, *Chem. Rev.* **1998**, *98*, 239 and references cited therein.
- [17] Rigaku, *CrystalClear Version 1.35*, Rigaku Corporation, **2002**.
- [18] Siemens, *SHELXTLTM Version 5 Reference Manual*, Siemens Energy & Automation Inc., Madison, Wisconsin, USA, **1994**.

Received: January 19, 2005

Published Online: June 22, 2005